Eur Biophys J (2006) 36:73–83
DOI 10.1007/s00249-006-0104-4

BIOPHYSICS LETTER

Spectrally resolved time-correlated single photon counting: a novel approach for characterization of endogenous fluorescence in isolated cardiac myocytes

D. Chorvat Jr · A. Chorvatova

Received: 21 April 2006 / Revised: 30 August 2006 / Accepted: 12 September 2006 / Published online: 11 October 2006
© EBSA 2006

Abstract A new setup for time-resolved fluorescence micro-spectroscopy of cells, based on multi-dimensional time-correlated single photon counting, was designed and tested. Here we demonstrate that the spectrometer allows fast and reproducible measurements of endogenous flavin fluorescence measured directly in living cardiac cells after excitation with visible picosecond laser diodes. Two complementary approaches for the analysis of spectrally- and time-resolved autofluorescence data are presented, comprising the fluorescence decay fitting by exponential series and the time-resolved emission spectroscopy analysis. In isolated cardiac myocytes, we observed three distinct lifetime pools with characteristic lifetime values spanning from picosecond to nanosecond range and the time-dependent red shift of the autofluorescence emission spectra. We compared obtained results to in vitro recordings of free flavin adenine dinucleotide (FAD) and FAD in lipoamide dehydrogenase (Lip-DH). The developed setup combines the strength of both spectral and fluorescence lifetime analysis and provides a solid base for the study of complex systems with intrinsic fluorescence, such as identification of the individual flavinoprotein components in living cardiac cells. This approach therefore constitutes an important instrumental advancement towards redox fluorimetry of living cardiomyocytes, with the perspective of its applications in the investigation of oxidative metabolic state under pathophysiological conditions, such as ischemia and/or metabolic disorders.

Keywords Fluorescence lifetimes · Spectroscopy · Flavin autofluorescence · Cardiac myocyte · TCSPC

D. Chorvat Jr
International Laser Centre, Bratislava, Slovak Republic

A. Chorvatova (✉)
Research Center, CHU Sainte-Justine,
3175 Cote Sainte Catherine, Montreal H3T 1C5, Canada
e-mail: alzbeta.chorvatova@recherche-ste-justine.qc.ca

A. Chorvatova
Department of Pediatrics, University of Montreal,
Montreal, Canada

Introduction

Fluorescence spectroscopy is represented by a wide spectrum of experimental methods that have been proven to be particularly important for the biological research. Owing to the technology advance in recent decades, a number of new promising fluorescence technologies have been introduced in combination with the light microscopy, allowing to specify a region of interest in the sample on a spatial scale in the (sub)-micron order. Fluorescence lifetime imaging (Wang et al. 1992; Gadella et al. 1993) and fluorescence microscopy with multi-wavelength detection (Dickinson et al. 2001) are just some of such examples, currently well implemented in a wide variety of instrumentation designs. Very recently, a new approach has been introduced to this family of methods, based on the simultaneous measurement of the fluorescence spectra and the fluorescence lifetimes. The spectrally resolved-fluorescence lifetime detection technique was already achieved on the base of time-correlated single photon counting (TCSPC), with either single-photon (Becker et al. 2002) or two-photon (Bird et al. 2004) excitation. It provides an extremely promising tool for quantitative

analysis of complex (e.g., intracellular) fluorescence signals, especially in regard to the prospect of its easy integration to laser-scanning confocal microscopy setups. Nevertheless, the potential of this technique in applications on single cell level, such as in cardiac myocytes, was still not fully achieved. Moreover, in spite of the broad range of applications of the fluorescence-lifetime microscopy, there is a very limited knowledge about the time-resolved parameters of the intrinsic flavin fluorescence measured in these cells.

In this contribution we describe the application of the spectrally resolved-fluorescence lifetime detection for the investigation of isolated cardiac cells. Our aim was to build an experimental setup allowing reproducible measurements of the low-intensity intrinsic fluorescence signals of living single cardiomyocytes under physiological conditions. We have therefore designed a novel micro-spectrometer based on the combination of inverted fluorescence microscope with TCSPC instrumentation, using picosecond laser diode excitation and simultaneous fluorescence decay detection on 16 spectral channels. We report the specifications of the developed setup and demonstrate the ability of the new instrument to perform cellular autofluorescence diagnostics in the flavin emission region.

Experimental

Cardiomyocyte isolation

Sprague–Dawley rats (13–14 week-old females, Charles River, Canada) were sacrificed by decapitation. All procedures were performed in accordance with Institutional Committee accredited by the Canadian Council for the Protection of Animals (CCPA). Left ventricular myocytes were isolated following retrograde perfusion of the heart with proteolytic enzymes (Chorvat et al. 2004). Myocytes were maintained in a storage solution at 4°C until used. Only cells that showed clearly defined striations were used in up to 10 h following isolation. Isolated cells were studied at room temperature in four-well chambers with coverslip-based slides (LabTech).

Solutions and drugs

The storage solution contained (in mmol/l): NaCl, 130.0; KCl, 5.4; $MgCl_2{\cdot}6H_2O$, 1.4; NaH_2PO_4, 0.4; creatine, 10.0; taurine, 20.0; glucose, 10.0; and HEPES, 10.0; titrated to pH 7.30 with NaOH. Basic external solution contained (in mmol/l): NaCl, 140.0; KCl, 5.4; $CaCl_2$, 2.0; $MgCl_2$, 1.0; glucose, 10.0; HEPES, 10.0; adjusted to pH 7.35 with NaOH. Basic intracellular solution contained (in mmol/l): KCl, 140.0; NaCl, 10; glucose, 10.0; HEPES, 10.0; adjusted to pH 7.25 with NaOH. Fluorescent probe Merocyanine 540 (MC540) from Molecular Probes-Invitrogen, USA was used at concentration 10^{-6} mol/l in redistilled water; 1,1′-diethyl-2,2′-carbocyanine iodide (DCI) from Aldrich, Canada was used at concentration 10^{-4} mol/l in EthOH; and 9,10-diphenylanthracene (DPA) from Fluka, Canada (stock solution prepared at 10^{-2} mol/l in cyclohexane) was analyzed at 10^{-8} M in EthOH. All other chemicals, including lipoamide dehydrogenase (LipDH) from porcine heart and flavin adenine dinucleotide (FAD), were from Sigma-Aldrich (Canada).

Definition of terms and data analysis

In our experiments, we typically collected a photon-counting histogram of spectrally resolved autofluorescence decay $P(\lambda_j, t_k)$. The histogram was measured simultaneously on 16 spectral channels, denoted as λ_j, and on 1,024 temporal channels denoted t_k. Fluorescence decay kinetics of cardiac myocyte autofluorescence was analyzed using a sum of three exponential terms, according to the model $I(\lambda_j, t)$ with the functional form:

$$I(\lambda_j, t) = I_{\text{baseline}} + \sum_{i=1}^{3} a_{i,j} \exp\left(-(t - t_0)/\tau_{i,j}\right)$$

where (t_0) is the variable zero-time shift, I_{baseline} fits the background intensity, and the amplitude (a_i) represent the fractional population of the molecules associated with each decay component i. Each lifetime component was thus assessed by examining its fluorescent lifetime (τ_i) and relative amplitude (a_i). The decay kinetics of FAD and LipDH in intracellular solution were analyzed analogically using one (FAD) or two (LipDH) exponential terms. For low-intensity fluorescence of diluted samples, an additional short-living component was necessary to include into the decay model to successfully fit the data. The amplitude of this component was strongly wavelength-dependent and similar component was observable also in the pure intracellular solution as the sharp peak with the maximum at the 495–513 nm spectral channel. For the analysis, the lifetime of this component was fixed to 100 ps. We attribute it dominantly to the 3,400 cm^{-1} line of Raman scattering in water that has to be centred at ~515 nm with the 438 nm excitation.

The time-resolved emission spectra (TRES) and area-normalized time-resolved emission spectra (TRANES) were constructed by summing the photons registered over a chosen time interval δt after a temporal delay Δt with respect to the channel k_{max}, where the maximal number of photon counts was detected:

$$\mathrm{TRES}(\lambda_j) = \sum_{k=(k_{max}+\Delta t)}^{(k_{max}+\Delta t+\delta t)} P(\lambda_j, t_k)$$

The TRANES spectra were subsequently background-substracted and area-normalized.

Data were analyzed using SPC-Image software (Becker & Hickl, Boston Electronics, USA), Origin 7.0 (OriginLab, USA) and custom-written procedures for data correction and analysis in visualization system Iris Explorer 5 (NAG, GB).

Results

Multispectral lifetime micro-spectroscopy of living cardiac cells

Newly designed experimental setup is based on combination of inverted microscope (Axiovert 200 M, Zeiss, Canada) with single-photon excitation by a picosecond diode laser and TCSPC hardware (see schematic representation at Fig. 1a). Picosecond diode lasers with emission lines at 375, 438, or 475 nm (BDL-series, Becker & Hickl, Boston Electronics, USA) are used as the excitation sources. These lasers with an output power up to ~1 mW provide pulse widths typically around 50 ps and allow user-selectable repetition frequency rate (20–80 MHz). In experiments on isolated cardiomyocytes, presented in this contribution, we have used mostly the 438 nm laser diode in order to excite the intrinsically fluorescing flavins close to the excitation maximum of FAD at 440–450 nm, corresponding also to the excitation maximum of the intrinsic fluorescence observed in cells (Chung et al. 1997; Huang et al. 2002; Chorvat et al. 2004).

The laser beam was first reflected to the sample through epifluorescence path of Axiovert 200-inverted microscope, creating slightly defocused elliptical spot at the objective focus, reaching typically 10–20 μm in diameter. The emitted fluorescence was then spectrally separated from the laser excitation using 395 nm dichroic filter and 397 nm long-pass filter (for excitation at 375 nm), 460 nm dichroic filter and 470 nm long-pass filter (for excitation at 438 nm) or 510 nm dichroic filter and 515 nm long-pass filter (for excitation at 475 nm). The filter cubes comprising the excitation/emission and dichroic filters were located in the microscope filter turret. A polarizer in magic-angle orientation was fitted in front of the detection system at the microscope output port, to avoid distortions of decay kinetics due to depolarization effects in the microscope optics. The emission was measured by a 16-channel multi-anode photomultiplier array (PML-16, Becker-Hickl, Boston Electronics, USA) attached to the 100 mm imaging spectrograph (Solar 100, Proscan,

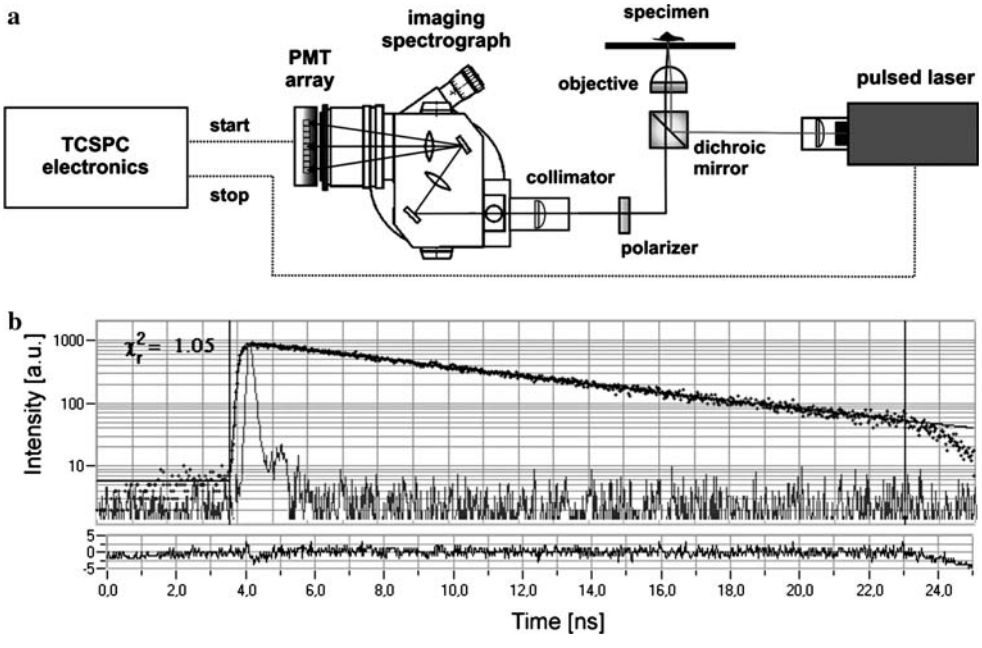

Fig. 1 **a** Schematic representation of the instrumental setup. **b** Temporal profile of the fluorescence emission of DPA in ethanol in one selected spectral channel detected by the PML-16 detector after excitation with 375 nm picosecond laser. Instrument response function (*grey line*) was estimated using DCI. *Points* measured data, *line* fitting curve denoting single-exponential decay convolved with instrument response

Germany). The PML-16 detector was running in the photon-counting regime and fed the TCSPC interface card SPC 830 (Becker-Hickl, Boston Electronics, USA) comprising of the discriminators, pulse-formation electronics, time-to-amplitude converter (TAC) and analogue-to-digital converter, all driven by the SPCM software. The card was synchronized-electrically by the laser diode driver in the reversed regime (stop signal was derived from the laser pulse). To ensure a sufficient time-window for observed autofluorescence kinetics, we selected a 20 MHz pulse repetition rate of the excitation laser. Accordingly, fluorescence decays were measured with 25 ns TAC time-base sampled by 1,024 points, thus each TAC channel was 24 ps wide. Detailed description and tests of the analogous TCSPC setup based on two-photon excitation were done by Bird et al. (2004). Here, we provide the most essential technical parameters of our instrument, describing its spectral and temporal performance.

To image the whole visible emission spectrum to the PMT array, the spectrometer was fitted with a grating (600 line-pairs/mm), providing the dispersion of 18 nm/mm. Since the channel width of the used PMT array was 1 mm, the value of 18 nm also corresponds to the rough spectral resolution of our system. The spectrometer was calibrated using the emission maxima of known reference dyes (such as DPA) and the water Raman peak. After calibration, we estimated the spectral range of our system to ~396–666 nm (channel mid-point values), with 16 equidistantly spaced spectral intervals 18 nm wide. The influence of higher orders of diffraction on the spectrograph linear dispersion was minimized using the dichroic and long-pass emission filters in the microscope, blocking completely the wavelengths below 400 nm from entering the spectrograph and the detector. Thus, we avoided the physical overlay of the signal from higher-order responses (<350 nm) over the first-order wavelength detection range (385–675 nm). We have not corrected our data either for spectral sensitivity of the detector, or for the spectral properties of the grating or dichroic filters. Therefore, the spectral profiles presented hereafter should be regarded as uncorrected emission spectra.

Due to the absorption characteristics of the microscope filter cubes, the instrument response function (IRF) of our setup could not be measured directly by laser-light scattering. For the estimation of instrument response profile we have therefore used the fluorescence of DCI in ethanol. This dye has reported a short excited state-lifetime of ~10 ps (Vetrova et al. 2005), with the emission peak at 625 nm. The typical width of the IRF using the 375 nm laser and the PML detector (Fig. 1b) was ~200 ps FWHM (full width in half-maximum), slightly exceeding the typical specifications of the convolved response functions of the detector itself (180 ps), the laser (60 ps) and the TCSPC electronics (8 ps). To test the precision of the setup in measurements at the nanosecond scale, we have recorded fluorescence kinetics of the fluorescence lifetime standard DPA in ethanol following 375 nm excitation (Fig. 1b). As expected, the observed decay was single exponential, with the estimated value of the fluorescence lifetime of 6.42 ± 0.12 ns, corresponding to the reported values of DPA lifetime ~ 6.1 ns (Poguet et al. 1989). The ability to resolve fast fluorescence kinetics was further tested by the measurement of fluorescence decay of MC540 in distilled water following excitation with 475-nm laser (data not shown). Estimated lifetime of MC540 after deconvolution using the routines in the SPC-Image software was 80 ps, which is in good agreement with the value of 90 ps obtained by femtosecond up-conversion technique (Bugar et al. 2002). This result indicates that a temporal resolution of ~100 ps can be readily attained by our setup using the deconvolution procedures.

A characteristic saw-form pattern was observed in all data scans recorded using the multi-anode PML-16 detector (Fig. 2a). This systematic effect was described by Becker et al. (2005) and reflects the variations of the temporal-shift of the detected photon histogram at different channels of the PMT array. Since the distortion thus introduced to the fluorescence decay (especially close to the leading edge of the excitation impulse) could substantially alter the observed spectra, we have developed a correction routine for elimination of this effect. In regard to the lack of availability of a single dye with the emission spectrum spanning over all spectral channels used for detection, three dyes were selected that emit fluorescence in either UV-blue (DPA), visible (MC540) or red (DCI) spectral regions. For each dye a spectrally resolved 2D plot of fluorescence decay (similar to Fig. 2a) was measured. Observed time-shifts were highly reproducible and equal for all fluorophores used, with the values specific for each spectral channel. Recorded data were therefore used to compute relative differences between the temporal points, given by the half of the leading edge of the observed fluorescence maxima in all spectral channels. Subsequently, a vector of negative temporal shifts was computed and used for the correction of the traces in the detected 2D plot. Example of the result of such data correction is shown at Fig. 2b.

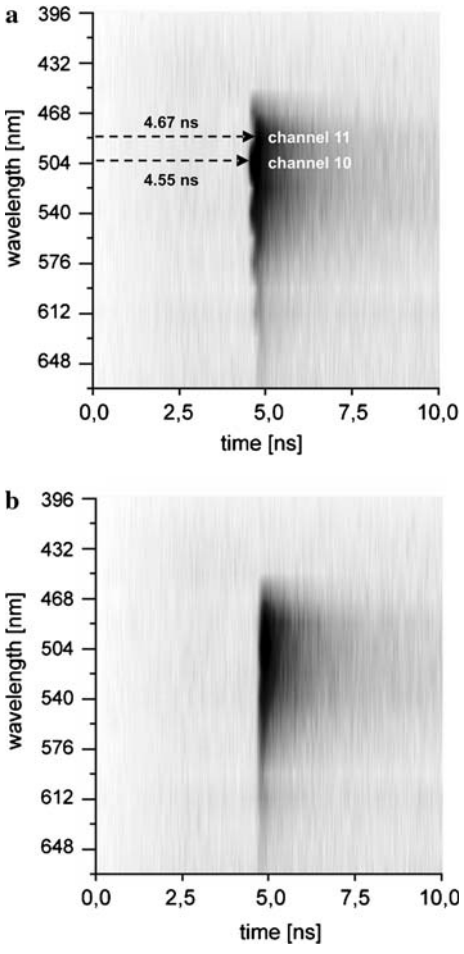

Fig. 2 Correction of the variable time shift of the cathode elements in the PML detector. **a** Original recording of the spectrally resolved TCSPC plot of the autofluorescence from single isolated cardiomyocyte excited by 438 nm laser. *Image* represents the 2D dependence of the fluorescence intensity on time (*X axis*) and wavelength (*Y axis*). The time shift values (indicated by *arrows*) in two representative channels (10,11) are shown. Time 0 ns was set arbitrarily using the delay parameters in the TCSPC electronics to suitably fit the range of the time-to-amplitude converter. **b** The same data as above after the time shift correction

Spectrally-resolved autofluorescence dynamics in cardiac myocytes

To demonstrate the application of the newly developed instrumental setup, we have recorded the spectrally-resolved TCSPC scans of the intrinsic fluorescence excited by violet (438 nm) picosecond laser diode in single isolated cardiomyocytes. The collection time was set to 2 min, due to the relative low signal intensity in comparison to cells labelled with standard fluorescence probes. Number of counts in channels of maximum intensity was typically around 1,000, with the background (measured in physiological solution and mostly attributable to ambient light and PMT dark signal) in the range of 10–50 counts per TAC channel. Total photon count of the autofluorescence signal on one spectral channel was typically in the range of 1–10×10^4 counts.

The autofluorescence spectral profile exhibit a broad emission peak in the range of 470–570 nm with spectral maximum at ~500–520 nm, corresponding to our previous findings linking this emission to flavins (Chorvat et al. 2005). The autofluorescence decay (Fig. 3) shows complex, multiple-exponential kinetics that need to be fitted with at least three-component exponential model to obtain acceptable χ^2 values (<1.2) (O'Connor and Phillips 1984). In addition to fluorescence lifetimes and their relative amplitudes, we have also considered a zero-time shift and *Y* offset as variable fitting parameters (see Experimental). However, after the correction of the zero-time shift of the PML detector using procedure described above, we were able to keep the zero-time shift fitting parameter fixed to the same value for all spectral channels. The results of the three-exponential lifetime analysis of the cardiac myocyte autofluorescence after excitation by 438 nm laser within the range of maximal intensity of the flavin emission are given in Table 1. The estimated fluorescence lifetime values indicate that the autofluorescence signal originate from molecular species with characteristic time-constants lying within three lifetime pools. The fastest component featured lifetime in the range of 0.15–0.20 ns, the intermediate lifetimes were estimated within the range of 0.5–1.0 ns; and the lifetime of the slowest decay component varied within 1.5–4 ns. The observed lifetime values and their relative amplitudes were dependent on both the excitation and emission wavelengths. The lifetimes of the intermediate and long components were prolonged and their relative amplitudes were slightly reduced at the red shoulder of the emission spectrum. Similar results were gathered following 475-nm excitation (data not shown).

Complete information about the spectral/temporal distribution of fluorescence intensity obtained by spectrally resolved TCSPC allows to analyze the data either in the form a set of multi-channel exponential decay series (a fluorescence lifetime analysis), or as a series of consecutive spectral profiles decaying in time. Therefore, as a complementary approach to the exponential decay analysis, we have also constructed the TRES representation of the detected data. In the monography on TCSPC technique, O'Connor and Philips (1984) stated that the TRES technique could yield to both qualitative and quantitative information that cannot be gleaned from the normal fluorescence spectra, even if extremely high optical resolution is

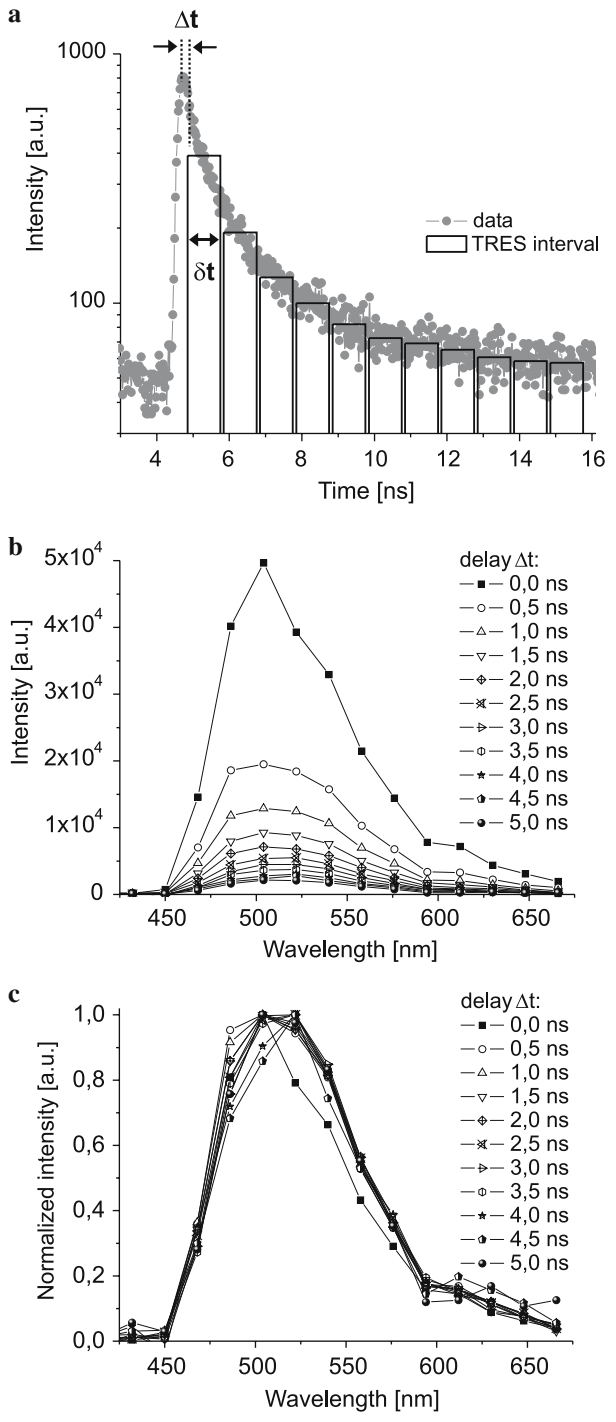

Fig. 3 Example of the flavin autofluorescence decay observed in rat cardiac myocytes after excitation by 438-nm laser. **a** Principle of the construction of the time-resolved emission spectra (TRES) from the data recorded by the spectrally-resolved TCSPC technique. Δt delay between the reference time (set to the maximum of the recorded intensity) and the beginning of the respective TRES channel; δt TRES channel duration. **b** Example of the TRES plot of cardiomyocyte autofluorescence with 0.5 ns resolution (δt = 0.5 ns, Δt = 0–5 ns with 0.5 ns step). **c** Normalized TRES plot of cardiomyocyte autofluorescence with 0.5 ns resolution

achieved. In our case, we have applied the TRES technique for a semi-quantitative spectral analysis of the time-resolved flavin autofluorescence in cardiac myocytes. We computed the summed-spectra from the original decay data in several consecutive temporal windows (Fig. 3a), starting at the point where the intensity reaches maximum. The width of the defined temporal windows was denoted δt, while the delays between the time reference (selected as the TAC channel where maximal intensity was detected) and the beginning of each window were denoted Δt. The delays Δt were set equidistantly with the interval equal to the window width δt. Due to the summation of the counts over multiple TAC-channels, the intensity of the TRES spectra increased respectively, when compared to the original recordings. The example of the TRES plot of flavin autofluorescence decay measured in cardiac myocytes with the temporal resolution of 0.5 ns is shown at Fig. 3b. It reveals rapid disappearance of the signal intensity within the first few nanoseconds, suggesting primary contribution of the nanosecond-lifetime components. The normalized TRES plot (Fig. 3c) shows spectral profile changes of the flavin cardiomyocyte autofluorescence in more details. The emission peak is broadening in time from 79 to 88 nm (FWHM) and simultaneously shifting the emission maximum from 504 to 522 nm. In the very first trace (Δt = 0 ns) an additional sharp peak at 504 nm is observable, with the characteristic decay time lying in the ps range. This peak is attributable mostly to the water Raman signal, because similar emission at 504 nm with short (ps) lifetime is also observable in pure extracellular solution at the same experimental conditions. Although the normalized TRES data in the form given at Fig. 3c could be used for quantitative comparison of the autofluorescence spectral profiles evolving in time, it is hard to judge whether the time-dependent wavelength shift of the emission maximum is due to continuous relaxation, or due to the presence of several emitting species with separate lifetimes. Therefore, we used an extended variant of TRES analysis, taking advantage of the area-normalized emission spectroscopy.

Time-resolved area-normalized emission spectroscopy of flavins in cardiac myocytes and in solution

For a successful analysis of the fluorescence decay data, at least a conceptual mathematical model is needed. In the case of simple decays with well-defined fluorescence lifetimes, such as in the mixtures of small number of fluorophores in solution, it is possible to resolve

Table 1 Fluorescence lifetime (τ_i) values of intrinsic flavin fluorescence, recorded following excitation by 438-pulsed picosecond lasers in isolated cardiomyocytes

Emission wavelength (nm)	τ_1 (ns)	τ_2 (ns)	τ_3 (ns)	a_1 (%)	a_2 (%)	a_3 (%)
495–513	0.17 ± 0.03	0.78 ± 0.18	1.48 ± 0.15	64.6 ± 2.2	22.4 ± 2.1	13.0 ± 1.5
513–531	0.15 ± 0.03	0.46 ± 0.13	1.70 ± 0.15	64.3 ± 2.0	22.0 ± 1.7	13.7 ± 1.2
531–549	0.18 ± 0.03	0.75 ± 0.13	2.10 ± 0.18	65.6 ± 1.9	21.0 ± 1.9	13.4 ± 0.9
549–567	0.20 ± 0.01	0.87 ± 0.13	2.81 ± 0.35	71.8 ± 1.7	17.2 ± 1.1	11.0 ± 1.3
567–585	0.18 ± 0.01	0.94 ± 0.15	3.67 ± 0.70	70.0 ± 2.6	19.4 ± 1.8	10.6 ± 1.2

Values were estimated by a three-exponential decay analysis within the emission range of 495–585 nm. Data are shown as mean ± SEM from $n = 5$ cells

the number and parameters of the decay components accurately by a multiple-exponential analysis. However, when an energy transfer or other non-exponential kinetics components are present, the data analysis could become complicated and is critically dependent on the proper formulation of the used mathematical model. Similar situation arises when we deal with an unknown molecules and/or molecules in an unknown environment such as the cellular autofluorescence—aiming to understand its molecular origins. In such case, one need to simultaneously analyze how many species are present in the sample and what model fits best their fluorescence kinetics.

In 2001, Koti and co-workers (2001) developed a method of TRANES—an area-normalized time-resolved emission spectroscopy—that allows to analyze the time-resolved spectroscopy data without any a-priori knowledge of the excited-state kinetics of the system under study. The TRANES method is based on the following principle: a spectrally-resolved fluorescence decays are measured, deconvolved, and the area-normalized spectra in the defined equidistant time delays of the deconvolved decay surface are constructed. Presence of the isosbestic point in the delayed traces indicates the existence of two (and only two) emitting species in the sample under the prerequisite that their fluorescence lifetimes and emission spectra are sufficiently different in the selected timescale. The origins of the observed TRANES components are highly dependent on the object under study, such as excited complex formation or multiple fluorophore emission. Here we therefore attempted to apply the TRANES technique to gain more insight into the possible molecular origins of the observed flavin autofluorescence decays in cardiac myocytes. We aimed to identify spectral properties of the autofluorescence components, as well to compare them to in vitro recording of FAD and LipDH in intracellular solution.

The deconvolution pre-processing suggested by Koti and co-workers (2001) is important not only for eliminating the intrinsic noise of the data obtained by photon counting, but mostly for the precise description of the very first moments of the decay. In our case, instead of data deconvolution, we tried to suppress the noise in the data by summation of photon counts in several consequent time channels analogically to the computation of TRES. More precisely, we computed the summed-spectra from the original decay data in equidistantly spaced temporal windows (similarly to Fig. 3a), and normalized them by the area under their spectral profile given by the integral of the intensity over all detected wavelengths. A strong prerequisite for TRANES analysis is that a complete spectra should be detected (Koti et al. 2001), what was fulfilled by our selection of the spectrograph wavelength range. To avoid distortions of the spectra after their normalization, a subtraction of a constant background present in all traces was necessary. The background data were taken from the very initial phase of the recordings, where no observable fluorescence signal from the sample was present. The width of the TRANES intervals we denoted analogically to the TRES case δt; and the delay between the time reference (channel with maximum counts) and the particular temporal window as Δt. The interval between the delays Δt was set equivalent to δt. We avoided the raising edge of the instrument response using only the decaying part of the data, thus reducing the convolution effects. However, cutting-off the data from the front edge of the recorded kinetics also limits our ability to resolve the early moments of the decay. Therefore, we were able to analyze only the processes with the characteristic time longer than the order of instrument response width (0.2 ns).

There are two main reasons for our decision why not to use the deconvolution routines. The first reason lies in our motivation to develop a fast, user-friendly routine for semi-quantitative spectral analysis of the TCSPC data with moderate (ns) time resolution that will be not dependent on the mathematical model and could be potentially implemented in the form of a real-time preview of the experimental data. Secondly, it was our endeavour to prevent artefacts resulting from

simultaneous analysis of the multiple-channel data by over-specified exponential series fitting. Manifested by the unavoidable oscillations in the fitting curve on some spectral channels, these were observed probably due to small systematic variations in the time shifts at the leading edge of the decay, persistent even after the applied corrections. These oscillations make the automatic fitting of the whole dataset complicated and user intervention is often needed for successful quantitative analysis or modeling of the decay. As indicated above, the effective time intervals sampled in the analysis of this type should not be in principle shorter than the instrument response width (O'Connor and Phillips, 1984). Given the FWHM value of our instrument response ~0.2 ns and the total temporal range of the observable signal (~0–10 ns), we have selected the TRANES interval width of $\delta t = 0.5$ ns to cover the nanosecond processes that could be observed in the recorded decay.

The TRANES spectra of cardiomyocyte flavin autofluorescence within 0.5–3 ns after the excitation impulse are presented at Fig. 4a. An isosbestic point located at 501 nm could be readily resolved, indicating that at least two emissive species are responsible for the cardiac autofluorescence signal. For comparison, we have generated the same TRANES analysis for the free FAD and for FAD cofactor bound in LipDH enzyme in vitro, in intracellular media-mimicking solution. The free FAD and FAD bound in mitochondrial-matrix enzymes (such as the LipDH, used here as a representative example) are considered to be the most apparent emission species in the cardiomyocyte autofluorescence following excitation with visible light (Huang et al. 2002; Romashko et al. 1998). The TRANES plots of FAD (Fig. 4b) show a single-component decay kinetics without any isosbestic point in the range of 0.5–3 ns. FAD has the emission maximum at 522 nm and single fluorescence lifetime of 2.47 ± 0.07 ns in the nanosecond range. Comparably, the TRANES spectra of LipDH (Fig. 4c) revealed no isosbestic point on the 0.5–3 ns scale. In contrast to FAD, the two-exponential decay analysis was necessary to successfully fit the data, and its emission maximum was shifted to 504 nm. The derived fluorescence lifetimes were $\tau_1 = 0.88 \pm 0.05$ ns and $\tau_2 = 4.14 \pm 0.11$ ns, with the relative amplitudes of 35 ± 1 and $65 \pm 1\%$, respectively. The lifetime and relative amplitude values of both LipDH and FAD given above were computed as a mean from three samples over three channels within the spectral range of 495–550 nm. For estimation of their spectral parameters we have compared the normalized spectral profiles of cardiomyocyte autofluorescence, FAD and LipDH, taken 1 ns after the excitation impulse (Fig. 5). The FWHM width of the spectral peaks was 66 nm for LipDH, 71 nm for FAD, and 88 nm for autofluorescence. The emission of FAD accounts very well for the

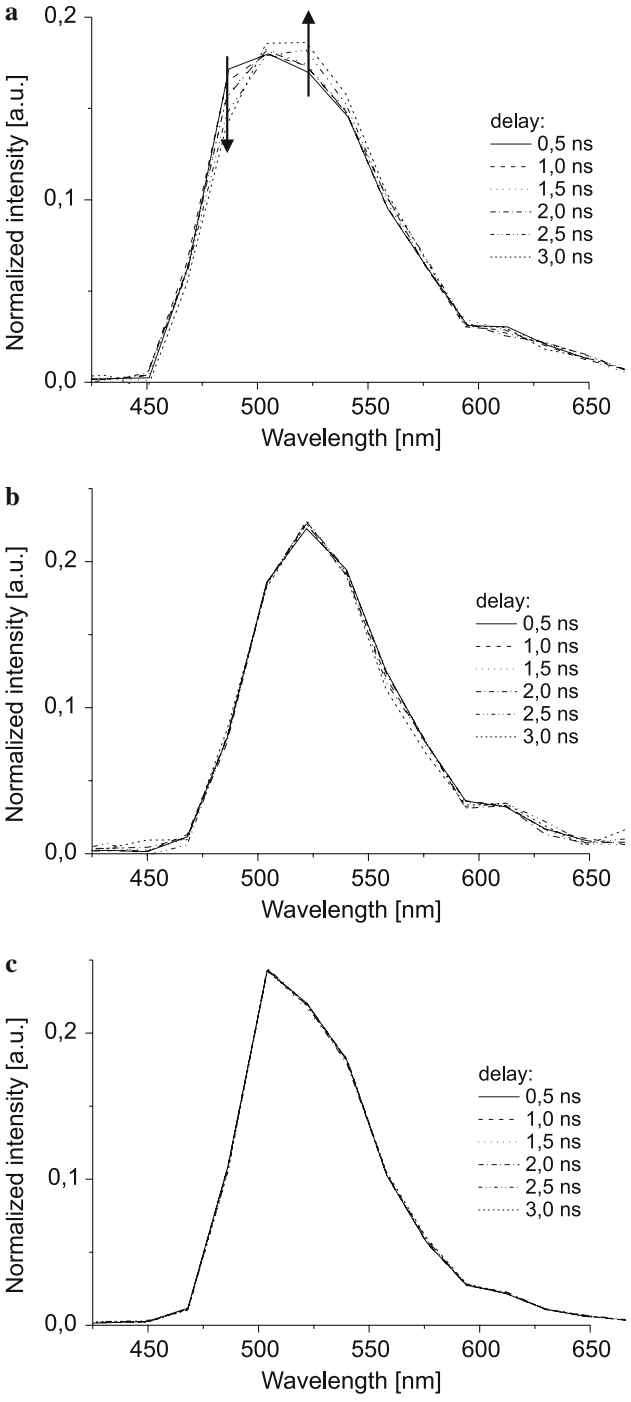

Fig. 4 Time-resolved, area-normalized emission (TRANES) spectra of **a** cardiomyocyte autofluorescence ($n = 8$ samples), **b** FAD fluorescence ($n = 3$ samples), and **c** LipDH fluorescence ($n = 3$ samples) in intracellular solution. Parameters: $\Delta t = 0.5$–3.0 ns, $\delta t = 0.5$ ns. Plots are constructed from mean values

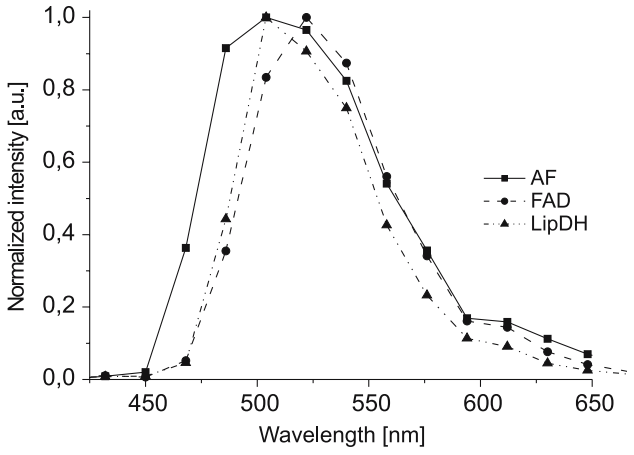

Fig. 5 Normalized spectra of cardiomyocyte autofluorescence, FAD and LipDH fluorescence in intracellular solution, measured 1 nanosecond after the excitation impulse ($\Delta t = 1$ ns) within the temporal window $\delta t = 0.5$ ns. Spectral profiles are selected from Fig. 4

long-wavelength part of the autofluorescence peak, while the emission of LipDH was blue-shifted with respect to the free flavin cofactor. However, the short-wavelength shoulder of the autofluorescence peak identified in cardiomyocytes was blue-shifted by another ~15 nm with respect to that of LipDH. This observation could be due to altered physio-chemical environment of the flavinoprotein molecules bound in the mitochondrial matrix compared to the intracellular solution; or as a consequence of the fact that we used LipDH isolated from bovine heart that could have slightly different spectral properties than the enzyme found in rat hearts.

Discussion

Our results revealed that the fluorescence lifetimes of flavin autofluorescence in cardiac myocytes are qualitatively in accordance with previously published data of the time-resolved FAD autofluorescence measured in vivo in human fundus (Schweitzer et al. 2004). However, the autofluorescence signal observed in cells is mostly the result of a summed signal from a broader range of different flavoproteins, whose relative presence is modulated by the cell physiological state (Chorvat et al. 2005). Moreover, regarding the published results on the time-resolved spectroscopy of FAD and flavinoproteins (e.g., Bastiaens et al. 1992; van den Berg et al. 2002), several channels of depopulation of the flavin excited state could be present in flavin-based proteins due to electron transfer from various amino-acid aromatic residues.

Flavin adenine dinucleotide in water solution displays a multicomponent fluorescence decay with two major lifetime pools. The first nanosecond component reflects the fluorescence of ''open'' molecule conformation. The second lifetime pool, observable at the picosecond range, is due to solvent relaxation in excited state and intramolecular electron transfer between flavin isoalloxazine ring and adenine in ''stacked'' FAD conformation (van den Berg et al. 2002; Chosrowjan et al. 2003). Fluorescence kinetics of the FAD moiety non-covalently bound in various flavoproteins exhibit similar behavior linked to the electron transfer between the isoalloxazine group and protein aromatic residues (such as those present in tryptophan, tyrosine or pyridine) in the enzyme catalytic center (Zhong and Zewail 2001). Moreover, the spectral relaxation observed in flavoproteins completes within 50 ps after excitation (Petushkov et al. 2003). The presence of these ultrafast decay components of FAD and LipDH in intracellular solution was checked in our samples using femtosecond fluorescence up-conversion technique (unpublished results). However, the integrated intensity of these components represents only a small fragment of the total photon counts detected on the nanosecond time-scales. Moreover, lifetimes lying in the picoseconds range are unresolvable under our experimental conditions due to the limited instrument response function width (~200 ps). This fact is even more pronounced in the case of faint fluorescence of diluted samples, where the fast (<100 ps) component was necessary to include into the decay model due to water Raman emission. All kinetic processes with the picosecond-range lifetimes occuring in the sample will contribute to the relative amplitude of this component, thus, with the described setup, it is not possible to achieve resolution below 100 ps. Therefore, flavoproteins with strongly quenched fluorescence will remain unresolved under our experimental conditions and the observed kinetics should be related to moderately fluorescent flavoproteins or the free flavins, all in spectrally relaxed form.

FAD fluorescence lifetimes measured with picosecond resolution were reported to be 0.3 ns (28%) and 2.8 ns (72%) (Visser 1984), while femtosecond resolution yields to four-component decay with the two dominant components of 2.7 ns (14%) and 7 ps (83%) (van den Berg et al. 2002). Regarding that lifetimes shorter than 0.2 ns could hardly be detected in our case, the lifetime value of 2.47 ns estimated for FAD in our case is in accordance with published results. Application of fluorescence lifetime analysis to the fluorescence kinetics studies of LipDH was performed, e.g. by Wahl et al. (1975) or Bastiaens et al. (1992). Both authors report that fluorescence lifetimes, as well

as their relative amplitudes, were temperature dependent. The authors used two or three-exponential model with the recovered lifetimes of 0.8 ns (46%) and 3.4 ns (54%) (Wahl et al. 1975); and 0.2 ns (5%), 1.3 ns (35%) and 2.5 ns (60%) (Bastiaens et al. 1992) at 20°C temperature. Our results estimated for LipDH at 24°C are comparable to these values.

Once complete information about the spectral distribution of intensity is known for the different time-delays of the fluorescence decay, one could project the data to the form of consecutive spectral profiles decaying in time. This point of view, representing the time-resolved emission spectroscopy approach, could serve as an alternative to the analysis of the same data by exponential series. In our case, we have used primarily a TRANES method, a recent extension to the family of the time-resolved spectroscopy approaches. This method was proved to be very effective for gathering of unambiguous results removing most of the intensity-related issues in the TRES analysis, thus allowing to analyze the decay data without assumptions about the mathematical model of their kinetics (Koti et al. 2001). We calculated the TRANES spectra of cardiac autofluorescence to identify how many spectral components are present in the observed decays. The TRANES analysis of cardiomyocyte autofluorescence with the nanosecond resolution show the shift of the emission maximum from 504 to 522 nm, accompanied with the presence of isosbestic point at 501 nm. Presuming that flavin emission is solely responsible for the observed signal, these data imply the presence of two distinct conformations and/or of molecular interactions of the FAD cofactors, either free or bound in various enzymes. The first emitting species with the maximum at ~485 nm and the corresponding lifetime in the order of ~1 ns could be resolved in the beginning of the decay, while second peak at ~522 nm could be resolved after several nanoseconds. It should be noted that each of the spectral components revealed in the TRANES spectra alone could have in principle multiple exponential decay kinetics, and/or it could be described by non-exponential model. The spectral shift by ~20 nm to longer wavelengths accompanied with the spectral peak broadening by ~10 nm could be due to the increased presence of free flavins (like FAD, Fig. 4b), which have distinct spectral and lifetime properties when compared to the flavin cofactors bound within the enzymes (LipDH, Fig. 4c). Due to its blue spectral shift and shorter fluorescence lifetime (corresponding to the second lifetime component revealed by exponential series analysis), we hypothesize that the 485-nm spectral component observable in TRANES spectra can be attributed to the FAD cofactor bound in some flavoprotein of the mitochondrial oxidative chain. The nanosecond lifetime of the red-shifted, slower-decaying component is comparable to the lifetimes of both isolated free FAD (2.47 ns), or the longer LipDH lifetime (4.14 ns), but the spectral maximum at 522 nm rather point to its origin in free FAD emission. Altogether, these results support our previous findings gathered by multispectral microscopy, that in the spectral range of 480–550 nm there exist two dominant emitting species in the cardiomyocyte autofluorescence with the emission maxima at ~500 and ~530 nm (Chorvat et al. 2005).

Successful identification of the spectral and lifetime fingerprints of the free FAD and FAD bound in enzymes in the oxidative chain of cardiac mitochondria at nanosecond and/or sub-nanosecond range could significantly improve the analysis of the flavin autofluorescence signal with the subsequent possibility to use the derived information for diagnostics of the cellular metabolism. The redox state can be studied using specific inhibitors of the respiratory chain, as described in our previous paper (Chorvat et al. 2005). Briefly, the rotenone, an inhibitor of LipDH can be used to block the electron transport chain at Complex I (Rocheleau et al. 2004) and prevent the NADH-linked flavin of LipDH from being oxidized (Romashko et al. 1998). The addition sodium cyanide, the blocker of electron transport at the level of the complex IV of the respiratory chain (Rocheleau et al. 2004; Kunz and Gellerich 1993) to cells pretreated with rotenone, allows to discriminate between flavoproteins tight to the respiratory chain below the complex I and the electron transfer flavoproteins (ETF). Addition of 2,4-dinitrophenol (DNP), the uncoupler of mitochondrial oxidation, is known to increase oxidized state of mitochondria (Romashko et al. 1998) and can be applied to promote generation of oxidized free flavins in cardiomyocytes.

Our results demonstrate that the designed setup for time-resolved emission micro-spectroscopy allows fast and reproducible measurements of complex patterns of spectrally resolved fluorescence decays directly in living cardiac cells. The method has the necessary sensitivity, as well as the temporal and spectral resolution allowing identification of various intrinsically fluorescing flavoproteins in cells under physiological conditions. The observed spectral/temporal behavior of flavin autofluorescence in cardiac myocytes proved to be a complex process, reflecting at least two different fluorescing molecular species present in the cardiac myocytes. Fluorescence lifetime analysis and area-normalized emission spectroscopy supports the hypothesis that free FAD and FAD bound in flavoprotein(s) of mitochondrial matrix are mostly responsible for the observed fluorescence emission.

Altogether, the novelty of the described setup is primarily in its possible application to measure fluorescence spectra and lifetimes from living cells under close-to-physiological conditions. In this regard, the spectrally- and time-resolved detection of flavin autofluorescence signals in cardiomyocytes, based on multidimensional time-correlated single photon counting, constitutes an important instrumental advancement towards quantitative redox fluorimetry of living cardiomyocytes, necessary for investigation of changes in mitochondrial oxidative metabolism under pathophysiological conditions, such as ischemia and/or metabolic disorders.

Acknowledgments This work was supported by Collaborative Linkage Grant LST.CLG.979836 from NATO to DC and AC; FRSQ (N 2948), CFI (N 9684) and CIHR (MOP 74600) grants to AC. We would like to thank V. Bassien-Capsa for cell isolation and A. Mateasik for programming of custom routines for data analysis.

References

Bastiaens PI, van Hoek A, Wolkers WF, Brochon JC, Visser AJ (1992) Comparison of the dynamical structures of lipoamide dehydrogenase and glutathione reductase by time-resolved polarized flavin fluorescence. Biochemistry 31(31):7050–7060

Becker W (2005) Advanced time-correlated single photon counting techniques. Springer, Berlin Heidelberg New York

Becker W, Bergmann A, Biskup C, Zimmer T, Klöcker N, Benndorf K (2002) Multi-wavelength TCSPC lifetime imaging. In: Ammasi Periasamy, Peter T So; (eds) Proc. SPIE - Multiphoton Microscopy in the Biomedical Sciences II, 4620:79–84

Bird DK, Eliceiri KW, Fan Ch-H, White JG (2004) Simultaneous two-photon spectral and lifetime fluorescence microscopy. Appl Opt 43(27):5173–5182

Bugar I, Chorvat D Jr, Palszegi T, Mach P, Urban J, Szöcs V (2002) Femto- and picosecond fluorescence dynamics of merocyanine 540: experiments and modeling. Femtochemistry and Femtobiology, Proceedings of 7th femtochemistry conference in Toledo, Word Scientific, Singapore, 298

Chosrowjan H, Mataga N, Taniguchi S, Tanaka F, Visser AJWG (2003) The stacked flavin adenine dinucleotide conformation in water is fluorescent on picosecond time scale. Chem Phys Lett 378:354–358

Chorvat D Jr, Bassien-Capsa V, Cagalinec M, Kirchnerova J, Mateasik A, Comte B, Chorvatova A (2004) Mitochondrial autofluorescence induced by visible light in single cardiac myocytes studied by spectrally resolved confocal microscopy. Laser Phys (14): 220–230

Chorvat D Jr, Kirchnerova J, Cagalinec M, Smolka J, Mateasik A, Chorvatova A (2005) Spectral unmixing of flavin autofluorescence components in cardiac myocytes. Biophys J 89(6): L55–57

Chung YG, Schwartz JA, Gardner CM, Sawaya RE, Jacques SL (1997) Diagnostic potential of laser-induced autofluorescence emission in brain tissue. J Korean Med Sci 12(2):135–142

Dickinson ME, Bearman G, Tilie S, Lansford R, Fraser SE (2001) Multi-spectral imaging and linear unmixing add a whole new dimension to laser scanning fluorescence microscopy. Biotechniques 31:1272–1278

Gadella TWJ Jr, Jovin TM, Clegg RM (1993) Fluorescence lifetime imaging microscopy (FLIM)—spatial resolution of microstructures on the nanosecond time-scale. Biophys Chem 48:221–239

Huang S, Heikal AA, Webb WW (2002) Two-photon fluorescence spectroscopy and microscopy of NAD(P)H and flavoprotein. Biophys J 82:2811–2825

Koti ASR, Krishna MMG, Periasamy N (2001) Time-resolved area-normalized emission spectroscopy (TRANES): a novel method for confirming emission from two excited states. J Phys Chem A 105:1767–1771

Kunz WS, Gellerich FN (1993) Quantification of the content of fluorescent flavoproteins in mitochondria from liver, kidney cortex, skeletal muscle, and brain. Biochem Med Metab Biol 50:103–110

O'Connor DV, Phillips D (1984) Time-correlated single photon counting. Academic, London

Petushkov VN, van Stokkum IHM, Gobets B, van Mourik F, Lee J, van Grondelle R, Visser AJWG (2003) Ultrafast fluorescence relaxation spectroscopy of 6,7-dimethyl-(8-ribityl)-lumazine and riboflavin, free and bound to antenna proteins from bioluminescent bacteria. J Phys Chem B 107:10934–10939

Poguet J, Mugnier J, Valeur B (1989) Correction of systematic phase errors in frequency-domain fluorometry. J Phys [E] 22:855–862

Rocheleau JV, Head WS, Piston DW (2004) Quantitative NAD(P)H/flavoprotein autofluorescence imaging reveals metabolic mechanisms of pancreatic islet pyruvate response. J Biol Chem 279:31780–31787

Romashko DN, Marban E, O'Rourke B (1998) Subcellular metabolic transients and mitochondrial redox waves in heart cells. Proc Natl Acad Sci USA 95:1618–1623

Schweitzer D, Hammer M, Schweitzer F, Anders R, Doebbecke T, Schenke S, Gaillard ER (2004) In vivo measurement of time-resolved autofluorescence at the human fundus. J Biomed Opt 9(6):1214–1222

van den Berg PAW, Feenstra KA, van Hoek A, Mark AE, Berendsen HJC, Visser AJWG (2002) Dynamic conformations of flavin adenine dinucleotide: simulated molecular dynamics of the flavin cofactor related to the time-resolved fluorescence characteristics. J Phys Chem B 106:8858–8869

Vetrova EV, Kudryasheva NS, Visser AJWG, van Hoek A (2005) Characteristics of endogenous flavin fluorescence of Photobacterium leiognathi luciferase and Vibrio fischeri NAD(P)H:FMN-oxidoreductase. Luminescence 20(3):205–209

Visser AJWG (1984) Kinetics of stacking interactions in flavin adenine dinucleotide from time-resolved flavin fluorescence. Photochem Photobiol (40):703–706

Wahl P, Auchet JC, Visser AJ, Veeger C (1975) A pulse fluorometry study of lipoamide dehydrogenase. Evidence for non-equivalent FAD centers. Eur J Biochem 50(2):413–418

Wang XF, Periasamy A, Herman B, Coleman DM (1992) Fluorescence lifetime imaging microscopy (FLIM): instrumentation and applications. Crit Rev Anal Chem 23:369–395

Zhong D, Zewail AH (2001) Femtosecond dynamics of flavoproteins: charge separation and recombination in riboflavine (vitamin B2)-binding protein and in glucose oxidase enzyme. Proc Natl Acad ci USA 98(21):11867–11872